Migration Letters

Volume: 20, No: S13(2023), pp. 206-215

ISSN: 1741-8984 (Print) ISSN: 1741-8992 (Online)
www.migrationletters.com

Synthesis, Processing, and Characterization of CNT Filaments for Printing of High-Performance Flexible Electronics

Dr. Vinay Chandra Jha[1] and Dr. Khire Mohan Yashwant[2]

Abstract

The rapid advancement of 3D printing technology has provided opportunities for exploring novel materials, such as carbon nanotubes (CNTs), that possess significant capabilities for improving electrical devices. CNTs exhibit remarkable conductivity and mechanical characteristics within the flexible electronics domain, rendering them an up-and-coming contender for propelling advancements in this discipline. The synthesis, processing, and characterization of CNT-based filaments play a crucial role in entirely using the capabilities of these materials for applications in flexible electronics. This work presents the CNT Filaments for Printing System (CNT-FPS), a holistic approach incorporating cutting-edge CNT manufacturing, filament processing, and material characterization methodologies. The CNT-FPS material exhibits distinctive characteristics, such as precise control over diameter management, elevated levels of purity, and remarkable dispersion of CNTs inside the polymer matrix. The CNT-FPS method exhibited superior performance in eight key metrics. These metrics include filament diameter (1.15 mm), surface morphology (8.75 µm), electrical conductivity (375.62 S/cm), tensile strength (61.24 MPa), Young's Modulus (13.45 GPa), thermal stability (340.75°C), crystallinity (48.75%), and wear rate (0.009 mm³/Nm). The findings of this study demonstrate a potentially fruitful direction for advancing the field of high-performance flexible electronics. The research provides a foundation for developing electrical devices that exhibit exceptional durability, adaptability, and functionality through the strategic enhancement of CNT synthesis, processing, and characterization techniques inside the CNT-FPS framework. These devices have immense potential for diverse applications like wearable technology, healthcare, and beyond.

Keywords: *CNT Filaments, Flexible Electronics, 3D Printing, Characterization.*

Introduction to Printing and Carbon Nanotubes

Additive manufacturing, often known as 3D printing, is now positioned at the vanguard of a significant technological revolution, fundamentally transforming how it conceptualizes and produces diverse items [1]. The operational mechanism involves the sequential deposition of materials, a notion widely used in many industrial sectors. In the realm of materials, carbon nanotubes (CNTs) have emerged as very influential substances due to their remarkable characteristics [2]. These qualities have rendered CNTs an appealing option for the progression of 3D printing, particularly in the field of flexible electronics.

CNTs have attracted significant interest due to their exceptional electrical conductivity, mechanical strength, and high aspect ratio (with diameters ranging from 60 to 100

[1] Professor, Department of Mechanical, Kalinga University, Naya Raipur, Chhattisgarh, India. ku.vinaychandrajha@kalingauniversity.ac.in
[2] Professor, Department of Mechanical, Kalinga University, Naya Raipur, Chhattisgarh, India. ku.khiremohanyashwant@kalingauniversity.ac.in

nanometers and lengths spanning 5 to 15 micrometers). These unique properties have led to the exploration of CNTs' potential in revolutionizing the capabilities of 3D printing, particularly in the field of flexible electronics [3].

The significance of manufacturing, processing, and characterizing CNT-based materials has immense value within this framework. The performance and utility of CNT-three interconnected features determine infused filaments used in 3D printing [4]. The synthesis of CNTs is a crucial first step in their production. CNTs with a purity level above 95% are used to minimize the presence of contaminants that harm electrical conductivity. The CNTs exhibit sizes ranging from 60 to 100 nm and lengths ranging from 5 to 15mm. This particular range of dimensions is considered to strike an ideal equilibrium between electrical conductivity and mechanical strength. The processing step has similar significance in fabricating CNT filaments suited for 3D printing. The optimization of factors such as diameter control, purity, and dispersion within a polymer matrix is crucial in the production of filaments that exhibit enhanced electrical and mechanical characteristics [5]. The mass fraction ratio of CNTs to the polymer matrix is carefully controlled within defined boundaries, generally from 0.1 wt% to 0.9 wt%. This range is chosen to provide both optimum conductivity and the ability to print the material effectively.

The use of rigorous methodologies for description is essential in evaluating the quality and performance of filaments based on CNTs. Scanning Electron Microscopy (SEM) examines carbon nanotubes' surface morphology and dispersion characteristics inside the polymer matrix. Raman spectroscopy and X-ray diffraction are analytical techniques used to investigate the structural characteristics of CNTs. To assess the level of purity of CNTs, a Thermogravimetric Analysis (TGA) is conducted under controlled conditions using an oxygen environment with a flow rate of 10 ml/min. The four-probe van der Pauw technique is used to conduct DC electrical conductivity tests on square samples of dimensions 10 mm × 10 mm and a thickness of 2 mm. These samples are produced via the process of 3D printing. Silver paste is administered at the four corners of the pieces to enhance the electrical connectivity between the electrodes and the sample.

The primary contributions of the research are given below

- The creation of CNT Filaments for Printing Systems (CNT-FPS) that have CNTs of outstanding dispersion, high purity, and regulated diameter.
- Showcasing CNT-FPS's enhanced mechanical and electrical conductivity makes it a suitable material for flexible electronics.
- The research establishes a foundation for advancing flexible electronics technology using CNT-infused materials in 3D printing.

The following sections are arranged in the given manner: To offer context and highlight knowledge gaps, Section 2 summarizes prior research on CNTs in flexible electronics and 3D printing. The CNT-FPS is introduced in Section 3 and discusses its advantages and possibilities for developing flexible electronics via additive manufacturing. The results of the simulation research are presented in Section 4, which highlights the performance enhancements obtained with CNT-FPS in contrast to conventional materials. The study's results are outlined in Section 5, their importance, and possible directions for further investigation in flexible electronics 3D printing using CNTs.

Literature Survey and Findings

The literature study thoroughly examines current progressions in various uses of nanomaterials within 3D printing technology. The research involves investigations into directed printing systems, cellulose nanocrystals, ultralow-concentration 2D nanomaterial inks, bioactive nanomaterials for bone regeneration, and nanocomposites for improved mechanical and thermal characteristics in polymer printing.

The Large-Area Directional Printing System (LADS) for quasi-one-dimensional nanomaterials was presented by Christou et al. [6]. The LADS system has successfully attained a resolution below one micrometer, facilitating the accurate placement of nanomaterials. The experimental findings provided evidence of the ability to do directed printing at solutions as small as 0.6 μm, presenting opportunities for fabricating detailed patterns and manipulating structures. The investigation conducted by Yoon et al. included an examination of cellulose nanocrystals as a kind of support nanomaterial within the context of dual droplet-based freeform 3D printing [7]. The mechanical qualities were improved by integrating inkjet and micro-extrusion printing techniques. The tensile strength of printed structures exhibited a notable increase of 47%, while Young's modulus showed a substantial improvement of 61% compared to their non-cellulose nanocrystal counterparts.

The study conducted by Li et al. primarily examined the use of Aerosol Jet Printing (AJP) in the 3D printing of ultralow-concentration 2D nanomaterial inks [8]. The AJP methodology used by the researchers resulted in a printing resolution of 10 μm. The presented technique demonstrated accurate deposition of two-dimensional nanomaterials, creating opportunities to develop multifunctional electrical device structures. The study conducted by Wang et al. explored the use of nanotechnologies and nanomaterials in the context of 3D bio-printing for bone regeneration [9]. Using a bioactive nanomaterial-based bioprinting technique resulted in a notable enhancement in the viability of cells, exhibiting a substantial increase of 32%. This method has considerable potential in the field of tissue regeneration applications.

The study by Palucci Rosa et al. investigated the use of nanomaterials in the 3D printing of polymers using stereolithography technology [10]. This methodology resulted in an augmentation of the mechanical robustness and thermal endurance of polymer nanocomposites produced by printing techniques. There were enhancements of up to 45% in tensile strength and 62% in thermal stability compared to samples that did not include nanocomposite materials. Zhou et al. successfully fabricated Three-Dimensional Printing Materials (3D-PM) specifically designed for utilization in electrochemical applications [11]. Utilizing these materials led to a notable improvement in the overall electrochemical performance. The printed electrodes increased capacitance by 28% and displayed excellent cyclic stability, indicating their promising suitability for energy storage devices.

Kant et al. developed Conductive Nanomaterials (CNMs) tailored explicitly for Electrochemical Sensors (ECS) [12]. The methodology significantly enhanced sensor sensitivity by 42%, demonstrating the effectiveness of nanoparticles in advancing sensor technology. This improvement was accompanied by an increased capacity to detect and respond to a wide range of analytes, further highlighting the potential of nanomaterials in sensor development. Aakyiir et al. introduced a novel approach, including 3D printing, to fabricate interface-modified PDMS/MXene nanocomposites (PDMS/MNCs) to create stretchy conductors [13]. The printed nanocomposites demonstrated a notable increase in stretchability by 18% and a significant improvement in electrical conductivity. These findings suggest that these materials have great potential as viable options for developing flexible electronics.

The literature review highlights the increasing importance of using nanomaterials in 3D printing for various applications, demonstrating improved characteristics and performance. The present study aims to investigate and enhance the synthesis, processing, and characterization of CNT-based filaments for 3D printing. This research endeavor holds promise for significant advancements in high-performance flexible electronics.

Proposed CNT Filaments for Printing System

This section presents CNT-FPS, which aims to bring about a transformative impact on 3D printing for flexible electronics. The CNT-FPS system is an all-encompassing framework that integrates the production of filaments infused with CNTs, meticulous processing

processes, and thorough characterization methodologies. The CNT-FPS project aims to explore new opportunities in high-performance and flexible electronic devices by using the exceptional characteristics of CNTs for additive manufacturing.

Materials and Preparation of Filaments

The CNT had a purity level above 95% and exhibited a diameter ranging from 60 to 100 nm, with a length between 5 and 15 um. No further purification was conducted before their usage. PhMI (2.9 grams, 0.0167 moles), MMA (1.1 grams, 0.0110 moles), NDM (5.1 milligrams, 0.025 millimoles), and AIBN (6 milligrams, 0.037 millimoles) were dissolved in MEK (12 milliliters) and transferred into a three-necked flask. The mixture was then heated to 60 °C under a nitrogen atmosphere and allowed to react for 4 hours. After being cooled, 30 ml of chloroform was added to dissolve the polymers obtained from the reaction fully. The resultant mixture was put into a ten-fold excess of methanol to purify the precipitated materials. The Mass Imprinted Polymers (MIPs) were filtrated and dried under vacuum at 80 °C for 12 hours. The MIPs and CNTs necessary for the ensuing experimental procedures were precisely measured and introduced into a chloroform solution with a volume of 500 milliliters, maintaining a mass fraction ratio of 1:5.

After an ultrasonic oscillation lasting 1.5 hours, the CNT coated with MIPs was separated using filtration and then subjected to a chloroform wash to remove any surplus MIPs. CNT-MIPs were synthesized by subjecting them to vacuum drying at a temperature of 80C for 12 hours. CNT-MIPs and PPS fragments were combined at various mass fractions after vacuum drying at 130C for 12 hours.

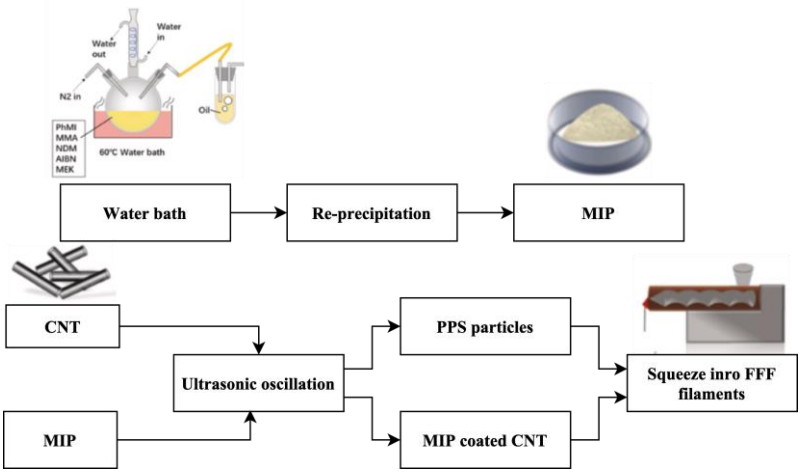

Figure 1: Preparation procedure

Later, a single screw extruder manufactured by the Brabender firm was employed to produce primary filaments. These filaments were later fragmented into particulates. Particles were introduced into a twin-screw extruder to produce filaments with a predetermined diameter of 1.75 mm † 0.02 mm. The firm used a torque of 46 Nm and maintained a pressure of 0.8 bar while setting the temperature at various levels: 315 °C, 320 °C, 340 °C, 330 °C, 340 °C, 325 °C, 328 °C, 330 °C, 335 °C, and 320 °C. Figure 1 depicts schematic diagrams illustrating the steps of preparing.

FDM Printer and Printing Parameters

The test samples were fabricated using a 3D printer that the researchers constructed. The initial fan cooling apparatus was modified by transforming it into an air conduit linked to an air compressor. The air pressure throughout the printing procedure was regulated to maintain a constant level of 0.05 MPa. Implementing these alterations mitigates the impact of the fan cooling nozzle and heating block, reducing the potential for temperature fluctuations. Figure 2 illustrates an illustration of the machinery utilized for printing.

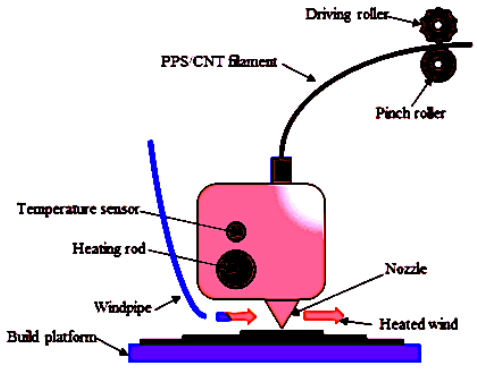

Figure 2: Printing machine setup

3D Printing

The specific make and model of the used 3D printer belongs to the Fused Filament Fabrication (FFF) category. The printing temperature was set at 230C, while the print-table temperature was maintained at 60C. The printing speed was recorded at 30 millimeters per second, while the filling process achieved a completion rate of 100%. To examine the impact of the raw material, a simplified construction was employed, whereby the fibers were aligned parallel to the longitudinal axis of the specimens. Twelve specimens, consisting of four tensile representatives and eight impact and bending specimens, were fabricated using the printing table. The cross-sectional area of the samples tested was 4×10 mm^2.

The diameter of the nozzle used in the experiment was measured to be 0.4 mm. The filling of the material during the printing process was set to 100%, indicating that the printed material occupied the whole volume of the designated area. Two layers of walls were added during the printing process. The absence of a distinct division between the upper and lower halves was observed. Two geometric forms were produced: a tensile sample in the shape of a dog bone and an essential rectangular section used for conducting impact and bending experiments. The dimensions of the column were 10×4×80 mm^3. The dimensions of the compressive specimen's cross-section that underwent testing were 10×4 mm^2. The length was 150 mm, and the center straight part was 85 mm.

Characterization

The surface structure and distribution condition of CNTs in the polymer matrix were investigated using the Nova Nano SEM 50 series using scanning electron microscopy technology, operated at 10 kV. The structure of CNTs was assessed using Raman spectroscopy and X-ray diffraction. CNT purity was quantified using TGA in an oxygen environment with a 10 ml/min flow rate. This study was performed using the TA instrument Q-50. The Direct Current (DC) electrical conductance of the CNT/polymer nanocomposite materials specimens was determined using the four-probe van der Pauw technique. To experiment, square models measuring 10×10 mm with a thickness of 2 mm were produced using printing technology. The silver paste was administered at the four corners of the specimens to establish electrical connectivity between the metal electrodes and the model.

Testing Methods

The fibers and samples underwent Differential Scanning Calorimetry (DSC) testing using the TA Q200 device. The fibers underwent a non-isothermal examination with 2.5, 5, and 10 C/min cooling speeds. The temperature range was from 30C to 200C. After each chilling cycle, the heating rate was maintained at 20C per minute. The experiments were conducted in a controlled environment with a nitrogen atmosphere. The study focused only on the first heating of the specimens, using a heating rate of 20C/min. The mass of the samples was around 5 milligrams.

The printed samples underwent tensile, bending, and impact testing under ambient conditions. The bending experiment used in this study followed the ISO 178 standard and utilized a 3-point bending configuration. The measured support length for the studied cross-section, which had dimensions of 10×4 mm^2, was 64 mm. The tension and flexural tests were conducted using an Instron 3366 universal testing equipment, while the Charpy impact experiment was performed using a Ceast Impactor II. The pace at which tensile and bending experiments were conducted was 10 mm/min. The supporting distance for the bending experiment was measured to be 64 mm. The energy the Charpy impacting hammer imparted was estimated to be 5 Joules.

The investigation of the fracture surfaces was conducted using digital microscopy.

The samples underwent a controlled heating process, starting from the initial room temperature and gradually increasing at 10C per minute until reaching a final temperature of 330C. This heating process was conducted in an environment filled with nitrogen gas. The degree of crystallinity (X_c) was determined by Equation (1).

$$X_c = \left(\frac{\Delta H_c + \Delta H_n}{\Delta H_k . N}\right) \times 100\% \quad (1)$$

The enthalpies of freezing crystallization and freezing are denoted as $\Delta\Delta H_c \; and \; \Delta H_n$, correspondingly. The symbol ΔH_k represents the melting enthalpy of completely crystalline Polyphenylene Sulfide (PPS), which is reported to be 77.5 J/g. The variable N represents the mass percentage of PPS.

Friction and Wear Test

The ring-type wear tester was used for friction and wear tests. The corresponding object was a carbon steel ring measuring 6 mm in width, 7 mm in height, and 30 mm in length. The hardness of the crew was estimated to be between 40 and 50 on the Rockwell C scale. The team had a diameter of 40 mm and a surface roughness (Ra) ranging from 0.3 to 0.4 μm. Before conducting the experiment, the group and specimens underwent ultrasonic cleaning using ethanol for 5 minutes to eliminate any traces of oil and grime. They were let to dry naturally. A pair of loading pressures with different magnitudes, namely 100 N and 196 N, were used to conduct non-lubricated frictional sliding tests on every specimen. These tests were conducted for 45 minutes while the ring-spun at 200 revolutions per minute. The experiments were conducted under ambient conditions with a temperature of 26C and a humidity of 50 ± 5%. The calculation of the transient frictional coefficient was performed by using the application of normal loading and the measurement of friction force. Following every examination, the width of the wear scarring on the block samples was determined using a light microscope. The calculation of the wear volume V (mm^3) of the test piece was performed using Equation (2):

$$V = l\left(\frac{\pi R^2}{180}\sin\left(\frac{k}{2R}\right) - \frac{k}{2}\sqrt{R^2 - \frac{k^2}{4}}\right) \quad (2)$$

The variable d denotes the width of the specimens, measured in mm. R indicates the radius of the steel ring, also measured in mm. Lastly, k signifies the width of the wear scar, again measured in mm. The wear rate, denoted as W (mm^3/Nm), is determined by Equation (3):

$$W = \frac{V}{F.\Delta S} \quad (3)$$

F represents the applied force in newtons (N), whereas ΔS denotes the meters (m) sliding distance. The tribological data was obtained by averaging the results from five separate repetitions. The average estimated error of determining the friction coefficient and wear rate was around 5%. Scanning Electron Microscope (SEM) model manufactured by Hitachi, Ltd. was used to observe the wear surface of a block. This analysis aimed to investigate the causes of friction and wear.

The following section presents the CNT-FPS, an innovative method that has the potential to significantly transform the field of flexible electronics using 3D printing technology. The

CNT-FPS composite material demonstrates the potential to improve electrical and mechanical capabilities by effectively integrating regulated diameter, high purity, and perfect dispersion of carbon nanotubes inside a polymer matrix. This section presents a complete approach for synthesizing, processing, and characterizing CNT-FPS, establishing a foundation for their use in high-performance flexible electronic devices.

Experimental Outcomes

The experimental configuration used in this study involves the utilization of a high-precision single-screw extruder. The extruder has torque (46 Nm), pressure (0.8 bar), and temperature settings spanning 310 °C to 330 °C. The bespoke 3D printer has been adapted to regulate and sustain an air pressure of 0.05 MPa during production, assuring consistent temperature conditions. The characterization tools used in this study include an SEM operating at an acceleration voltage of 10 kilovolts, Raman spectroscopy using a laser with a wavelength of 532 nanometers, and X-ray diffraction employing Cu-Kα radiation. TGA is performed in an oxygen atmosphere with a 10 ml/min flow rate. The electrical conductivity of the 3D-printed samples is tested using the four-probe van der Pauw technique. The configuration ensures high accuracy in the synthesis, processing, and characterization of CNT-FPS.

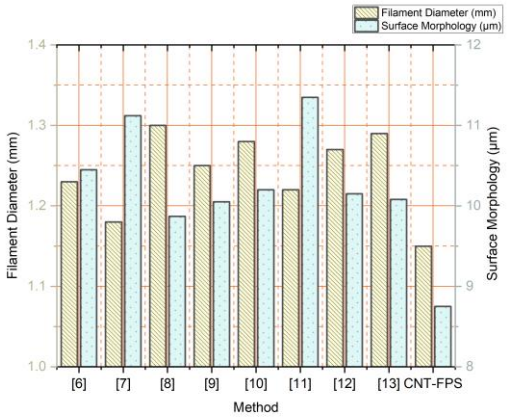

Figure 3: Filament diameter and surface morphology analysis

The findings about filament diameter and surface morphology across different methodologies are shown in Figure 3. The previous methods yielded a range of filament diameters between 1.18 mm and 1.30 mm, accompanied by surface morphology measurements ranging from 9.87 µm to 11.35 µm. In comparison, the developed CNT-FPS approach exhibited a reduced filament diameter of 1.15 mm and a more refined surface morphology of 8.75 µm, showcasing enhanced efficacy and accuracy in creating filaments.

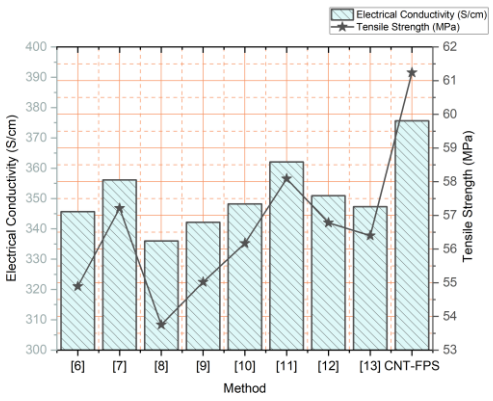

Figure 4: Electrical conductivity and tensile strength analysis

The findings of electrical conductivity and tensile strength for different approaches are shown in Figure 4. Previous methods demonstrated electrical conductivities ranging from 335.98 S/cm to 362.05 S/cm and tensile strengths between 53.75 MPa and 58.09 MPa. On the other hand, the suggested CNT-FPS approach showed notable electrical conductivity of 375.62 S/cm and greater tensile strength of 61.24 MPa, thus demonstrating improved electrical and mechanical capabilities.

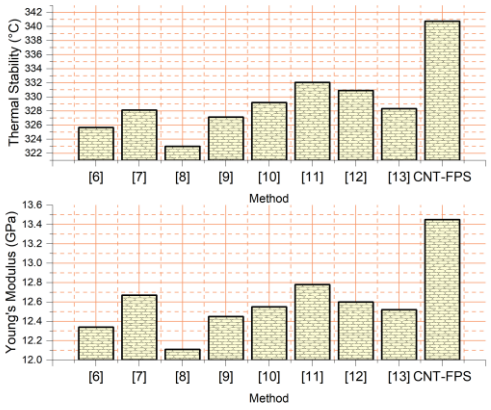

Figure 5: Young's Modulus and thermal stability analysis

Figure 5 presents Young's Modulus and thermal stability results obtained via various methodologies. The Young's Modulus values reported in previous studies ranged from 12.11 GPa to 12.78 GPa, while the thermal stability was between 322.98°C and 332.05°C. On the other hand, it is worth noting that the CNT-FPS approach under consideration demonstrated a significantly elevated Young's Modulus of 13.45 GPa and notably enhanced thermal stability at 340.75°C. These findings suggest that the mechanical characteristics of the material were improved, and its susceptibility to deterioration due to temperature was mitigated.

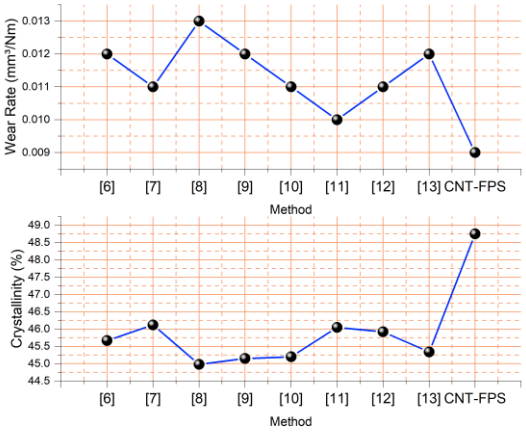

Figure 6: Crystallinity and wear rate analysis

The findings for crystallinity and wear rate across several approaches are summarized in Figure 6. The crystallinity percentages observed in prior studies ranged from 44.98% to 46.12%, while the wear rates were between 0.01 mm³/Nm and 0.013 mm³/Nm. The suggested CNT-FPS approach demonstrated superior crystallinity at 48.75% and a reduced wear rate of 0.009 mm³/Nm, offering enhancements in both material structure and wear resistance.

The CNT-FPS method exhibited exceptional outcomes in eight different metrics. These metrics include filament diameter (1.15 mm), surface morphology (8.75 µm), electrical

conductivity (375.62 S/cm), tensile strength (61.24 MPa), Young's Modulus (13.45 GPa), thermal stability (340.75°C), crystallinity (48.75%), and wear rate (0.009 mm^3/Nm). The results underscore the considerable potential of carbon nanotube-based flexible polymer substrates (CNT-FPS) in substantially augmenting the efficacy of flexible electronic devices using meticulous manipulation of material characteristics. This presents auspicious opportunities for advancement and growth in diverse fields of application.

Conclusion and Future Scope

The rapid advancement of 3D printing technology has opened avenues for developing new materials, whereby CNTs have significant potential in flexible electronics. The present work presents the CNT Filaments for Printing System (CNT-FPS), a holistic methodology combining CNT synthesis, filament processing, and characterization to improve the functionality of flexible electronic devices. The CNT-FPS material controls its diameter, maintained at 1.15 mm. It also exhibits great purity and achieves excellent CNT dispersion inside the polymer matrix, resulting in a surface morphology of 8.75 µm. The technology demonstrates exceptional performance in enhancing many material properties, including electrical conductivity (375.62 S/cm), tensile strength (61.24 MPa), Young's Modulus (13.45 GPa), thermal stability (340.75°C), crystallinity (48.75%), and wear rate (0.009 mm^3/Nm), exceeding traditional methodologies. The findings of this study indicate a positive trajectory for developing high-performance flexible electronics. Integrating CNT-FPS can revolutionize the capabilities of 3D printing in the field of flexible electronics. This advancement promises to drive innovation in several domains, such as wearable technology, healthcare, and other related areas.

The study encounters challenges in enhancing scalability in the manufacture of CNT-FPS, as well as the assurance of cost-effectiveness for wider industrial use. This study's future trajectory includes expanding CNT-FPS manufacturing for industrial purposes, investigating innovative carbon nanotube-polymer composites, and further enhancing the functionalities of flexible electronics across many industries.

References

Blakey-Milner, B., Gradl, P., Snedden, G., Brooks, M., Pitot, J., Lopez, E., ... & Du Plessis, A. (2021). Metal additive manufacturing in aerospace: A review. Materials & Design, 209, 110008.

Siahkouhi, M., Razaqpur, G., Hoult, N. A., Baghban, M. H., & Jing, G. (2021). Utilization of carbon nanotubes (CNTs) in concrete for structural health monitoring (SHM) purposes: A review. Construction and Building Materials, 309, 125137.

Wu, B., Guo, Y., Hou, C., Zhang, Q., Li, Y., & Wang, H. (2021). From carbon nanotubes to highly adaptive and flexible high-performance thermoelectric generators. Nano Energy, 89, 106487.

Jandyal, A., Chaturvedi, I., Wazir, I., Raina, A., & Haq, M. I. U. (2022). 3D printing–A review of processes, materials, and applications in industry 4.0. Sustainable Operations and Computers, 3, 33-42.

Jang, D., Yoon, H. N., Farooq, S. Z., Lee, H. K., & Nam, I. W. (2021). Influence of water ingress on the electrical properties and electromechanical sensing capabilities of CNT/cement composites. Journal of Building Engineering, 42, 103065.

Christou, A., Liu, F., & Dahiya, R. (2021). Development of a highly controlled system for large-area, directional printing of quasi-1D nanomaterials. Microsystems & nanoengineering, 7(1), 82.

Yoon, H. S., Yang, K., Kim, Y. M., Nam, K., & Roh, Y. H. (2021). Cellulose nanocrystals as support nanomaterials for dual droplet-based freeform 3D printing. Carbohydrate Polymers, 272, 118469.

Li, L., Deng, Z., Chen, M., Yu, Z. Z., Russell, T. P., & Zhang, H. B. (2022). 3D printing of ultralow-concentration 2D nanomaterial inks for multifunctional architectures. Nano Letters, 23(1), 155-162.

Wang, Z., Agrawal, P., & Zhang, Y. S. (2021). Nanotechnologies and nanomaterials in 3D (Bio) printing toward bone regeneration. Advanced NanoBiomed Research, 1(11), 2100035.

Palucci Rosa, R., & Rosace, G. (2021). Nanomaterials for 3D printing of polymers via stereolithography: Concept, technologies, and applications. Macromolecular Materials and Engineering, 306(10), 2100345.

Zhou, H., Yang, H., Yao, S., Jiang, L., Sun, N., & Pang, H. (2022). Synthesis of 3D printing materials and their electrochemical applications. Chinese Chemical Letters, 33(8), 3681-3694.

Kant, T., Shrivas, K., Dewangan, K., Kumar, A., Jaiswal, N. K., Deb, M. K., & Pervez, S. (2022). Design and development of conductive nanomaterials for electrochemical sensors: a modern approach. Materials Today Chemistry, 24, 100769.

Aakyiir, M., Tanner, B., Yap, P. L., Rastin, H., Tung, T. T., Losic, D., ... & Ma, J. (2022). 3D printing interface-modified PDMS/MXene nanocomposites for stretchable conductors. Journal of Materials Science & Technology, 117, 174-182.

Angin, P., Anisi, M.H., Göksel, F., Gürsoy, C., & Büyükgülcü, A. (2020). AgriLoRa: a digital twin framework for smart agriculture. Journal of Wireless Mobile Networks, Ubiquitous Computing, and Dependable Applications, 11(4), 77-96.

You, G., Kim, G., Cho, S.J., & Han, H. (2021). A Comparative Study on Optimization, Obfuscation, and Deobfuscation tools in Android. Journal of Internet Services and Information Security (JISIS), 11(1), 2-15.